ELSEVIER

Journal of Alloys and Compounds 404–406 (2005) 191–194

Journal of ALLOYS AND COMPOUNDS

www.elsevier.com/locate/jallcom

Neutron diffraction study of Ho_5YFe_{23} and $Ho_5YFe_{23}D_{16}$ deuteride

J. Ostoréro[a,*], V. Paul-Boncour[a], F. Bourée[b], G. André[b]

[a] *CNRS, Lab. de Chimie Metallurgique des Terres Rares, 2 Rue Henri Dunant, UPR 209, 94320 Thiais Cedex, France*
[b] *LLB, CEA Saclay, 91191 Gif sur Yvette cedex, France*

Received 6 September 2004; accepted 16 September 2004
Available online 18 July 2005

Abstract

Neutron diffraction experiments (LLB) were performed on $Ho_5YFe_{23}D_z$ and its parent alloy Ho_5YFe_{23} to determine the localization of deuterium atoms, precise their magnetic structures and compare to previously determined low magnetic field magnetization properties of $Ho_{6-x}Y_xFe_{23}H_z$ ($0 \leq x \leq 6$; $z = 16$). In both alloy and deuteride, the Fe moments are coupled ferromagnetically to each other and antiferromagnetically to the rare-earth. At low temperature, the magnetic moment of Ho is slightly less than its free ion value (9.2 μ_B at.$^{-1}$ versus 10 μ_B at.$^{-1}$). A decrease of the magnetic Ho–Fe exchange interaction is observed in relation to the increase of atomic distances upon hydrogenation. In comparison to parent alloy, absorption of hydrogen leads to a decreasing T_{comp}, a strong increase of the Fe magnetic moment. A canting model gives a slightly better fit of the neutron data as compared to a pure ferrimagnetic model. The mean canting angle is small ($\theta < 10°$) in agreement with Herbst and Croat refined-Néel molecular field model used in the discussion of the magnetization experiments.
© 2005 Elsevier B.V. All rights reserved.

Keywords: Neutron diffraction; Hydrogen storage materials; Magnetically ordered materials

1. Introduction

Among rare-earth (R)–transition metal (T) intermetallic compounds, iron-based alloys R_6Fe_{23} (R = Gd–Yb) with a magnetic compensation temperature T_{comp} present a great interest for applications, e.g. thin films for high density magnetic and magnetooptic information recording media. In bulk materials, absorption of hydrogen leads easily to the formation of hydrides of formula $R_6Fe_{23}H_z$ ($z < 18$ under ordinary conditions) [1].

Most hydrides of the intermetallic compounds R_6Fe_{23} (R = Ho, Y) retain the cubic *Fm*3*m* host structure, R being located in site (24e), Fe occupying the four distinct positions (4b, 24d, $32f_1$ and $32f_2$) and H occupying the available interstitial sites [1,2]. We presented recently low magnetic field results of yttrium-substituted Ho_6Fe_{23} intermetallic alloys and their corresponding hydrides $Ho_{6-x}Y_xFe_{23}H_z$ ($x = 0.5$, 1; $z = 16$) [3,4]. The "non-magnetic" yttrium-substitutes Ho on the unique rare-earth site for both compounds. The experimental results were interpreted on the basis of Fe moments coupled ferromagnetically to each other and antiferromagnetically to the rare-earth within the frame of Herbst and Croat refined-Néel molecular field model [5] which takes into account canted magnetic structures present in R–T compounds.

In order to precise the magnetic structures, the influence of insertion of hydrogen and yttrium substitution on the magnetic properties and determine the location of hydrogen atoms, we performed neutron diffraction experiments (LLB Saclay) as a function of temperature on $Ho_5YFe_{23}D_z$ ($z = 0$, 16) compounds. It is to be noted that the yttrium-substitution rate $x = 1$ corresponds to the most canted magnetic structures observed in the magnetization experiments [3].

2. Experimental

Single phase Ho_5YFe_{23} and its deuteride $Ho_5YFe_{23}D_z$ ($z = 16 \pm 0.5$) were synthesized as indicated in Ref. [3], with cubic lattice constants of 1.20397 and 1.24394 nm for alloy and deuteride, respectively.

The neutron powder diffraction (NPD) patterns of the deuterides have been registered at 290 K on the 3T2 diffractometer and from 1.5 to 290 K on the G4.1 diffractometer at the

* Corresponding author. Tel.: +33 1 49 781 174; fax +33 1 49 781 203.
E-mail address: ostorero@glvt-cnrs.fr (J. Ostoréro).

0925-8388/$ – see front matter © 2005 Elsevier B.V. All rights reserved.
doi:10.1016/j.jallcom.2004.09.094

Laboratoire Léon Brillouin (LLB) at Saclay. For the 3T2 experiments, the wavelength was 1.225 Å and the angular range $6^\circ < 2\theta < 125^\circ$ with a step of 0.05°. For the G4.1 experiments, the wavelength was 2.427 Å and the angular range was $2^\circ < 2\theta < 82^\circ$ with a step of 0.1°. All the XRD and NPD were refined with the Rietveld method, using the Fullprof program [6]. It is to be noted that the 3T2 and G4.1 experiments performed on $Ho_5YFe_{23}D_{16}$ and its parent alloy Ho_5YFe_{23} present a very similar behaviour, and only the refinement results concerning the alloy will be given.

3. Results and discussion

3.1. Neutron diffraction experiments at 290 K on 3T2

Fig. 1 shows the NPD 290 K data of 3T2 for $Ho_5YFe_{23}D_{16}$. The refined lattice parameters, atomic coordinates, occupation numbers and thermal factors are given in Table 1. $Ho_5YFe_{23}D_{16}$ retains the same cubic *Fm*3*m* structure as its parent alloy, with a strong increase of the cubic lattice constant upon hydrogenation: $\Delta a/a = 3.3\%$ and $\Delta V/V = 9.3\%$.

The deuterium atoms occupy partially the tetrahedral $32f_3$, $96j_1$, $96j_2$ and 96k sites. This deuterium distribution is close to that previously observed in unsubstituted $Ho_6Fe_{23}D_{15.7}$ [7,8]. This indicates that the yttrium substitution, at least at this substitution rate, has no sensitive effect on the hydrogen distribution in the Ho_6Fe_{23} lattice: particularly very few or no deuterium atom could be placed in the octahedral 4a site, otherwise this would result in unrealistic parameters for this atom as was previously observed for $Ho_6Fe_{23}D_{15.7}$. In agreement with the increase of lattice parameter, a strong increase of the interatomic distances is observed upon hydrogenation, e.g. the mean distance between an (Ho, Y) atom and its 13 Fe neighbours atoms is 0.3045 nm in the alloy and 0.3176 nm in the deuteride.

3.2. NPD experiments on G4.1 versus temperature

The 1.5 K NPD spectrum measured on G4.1 is plotted in Fig. 2 for the deuteride $Ho_5YFe_{23}D_{16}$. The alloy and deuteride keep the same cubic structure in the whole temperature range 1.5–290 K. The thermal expansion of the lattice volume is reported in Fig. 3. It is obvious that hydrogen absorption decreases the thermal expansion coefficient. A fit of this coefficient using the analytical relations for phonons contribution ([9] and references therein) allowed us to calculate the Debye temperature parameter which is higher for the deuteride as compared to the parent alloy: 261 and 204 K, respectively.

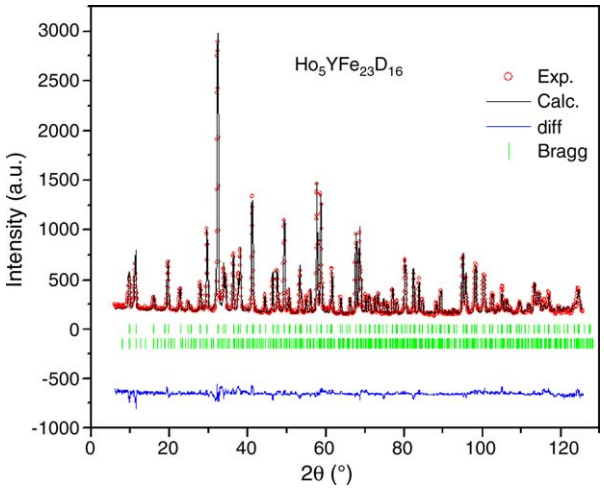

Fig. 1. $Ho_5YFe_{23}D_{16}$ room temperature 3T2 neutron diffraction pattern. The full curve is the calculated intensity pattern, the vertical lines correspond to the Bragg reflections and the residuals are plotted at the bottom of the figure.

3.3. Magnetic structures

When $2\theta < 60^\circ$, the intensities of the NPD peaks decrease sharply when the temperature increases. This is related to the influence of the magnetism of the compound which decreases when temperature increases towards the Curie point. In order to get more precise informations on the magnetic structures of the hydride, the 3T2 more finely refined crystalline parameters are used as the nuclear basis for the Fullprof refinement of the temperature NPD data obtained on G4.1 (Fig. 2).

The refinement results for the site atomic magnetic moments at 1.5 K are given in Table 2 for Ho_5YFe_{23} and

Table 1
Structural parameters of Ho_5YFe_{23} and $Ho_5YFe_{23}D_{16.3}$ (parenthesis) determined at 290 K from 3T2 NDP

Atom	Site	*x y z*	Alloy	Deuteride	Biso	*n*
Ho	24e	*x* 0 0	$x = 0.206$ (1)	$x = 0.209$ (6)	0.644 (8), 0.626 (6)	0.8333
Y	24e	*x* 0 0				0.1666
Fe 1	4b	1/2 1/2 1/2			0.619 (3), 0.882 (7)	1
Fe 2	24d	0 1/4 1/4				1
Fe 3	$32f_1$	*x x x*	$x = 0.176$ (2)	$x = 0.175$ (3)		1
Fe 4	$32f_2$	*x x x*	$x = 0.378$ (1)	$x = 0.370$ (9)		1
D 1	4a	0			–	∼0
D 2	$32f_3$	*x x x*		$x = 0.0969$ (6)	0.902 (0)	0.225
D 3	$96j_1$	0 *y z*		$y = 0.137$ (9), $z = 0.334$ (4)		0.0528
D 4	$96j_2$	0 *y z*		$y = 0.0946$, $z = 0.374$ (1)		0.036
D 5	96k	*x x z*		$x = 0.159$ (7), $z = 0.0304$ (5)		0.0058

Quality of fit $R_{nuc} = 8.46\%$ (deuteride) and 4.55% (parent alloy).

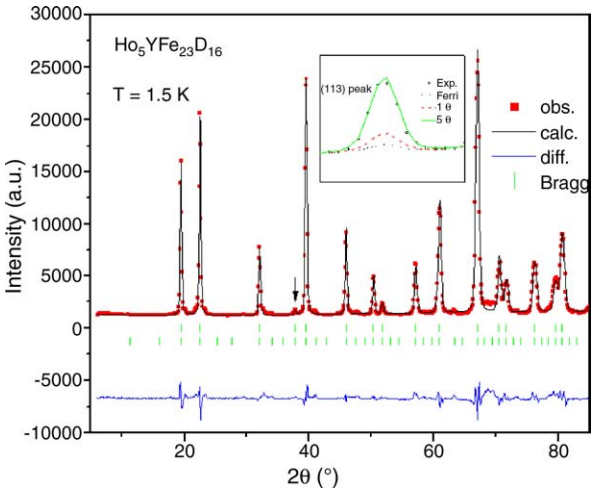

Fig. 2. $Ho_5YFe_{23}D_{16}$ neutron diffraction G4.1 pattern at 1.5 K. Inset: zoom of the (1 1 3) peak (arrow). The solid line correspond to "free canting" angles in the sublattices, the dashed curve to canting of the Ho sublattice only, the dotted line to ferrimagnetic model (see text).

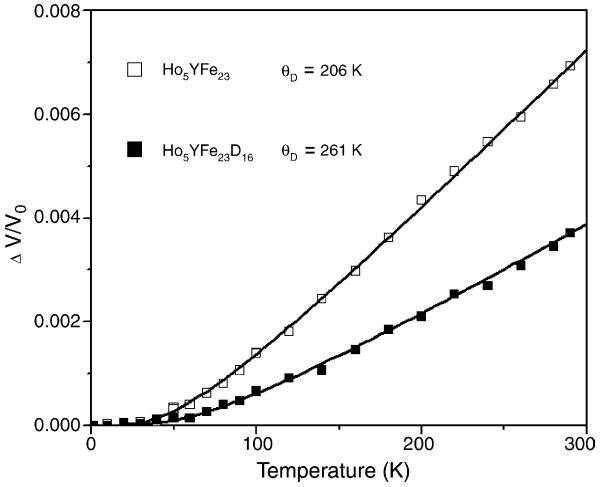

Fig. 3. Temperature variation of $\Delta V/V(T=0)$ for $Ho_5YFe_{23}D_{16}$ and Ho_5YFe_{23}. The solid lines correspond to calculated values (Ref. [9]) for indicated Debye temperature θ_D parameters.

$Ho_5YFe_{23}D_{16}$. The Fe moments coupled ferromagnetically to each other and antiferromagnetically to the Ho moments. Three different magnetic models were used during the refinement: a ferrimagnetic model, a canting model where the canting is observed for Ho only, and a "free canting" model where the moments of the magnetic atoms in the five sublattices are situated in the xOz plan.

The ferrimagnetic model is the one which requires the less number of parameters. A good fit could be obtained only with a minimum of five distinct moments corresponding to the five sublattices locations of the atoms: one for Ho and four for Fe atoms. As indicated in Table 2, the quality of fit is good and the calculated bulk magnetic moment of the deuteride is close to its experimental value 8.5 μ_B (f.u.)$^{-1}$ measured at 4.2 K.

We tried to quantify the canting observed previously in hydride of $Ho_{6-x}YFe_{23}$ alloys [3,4] by first adding a z component for the Ho moment in the Fullprof refinement. Only a small z component could be obtained for an equivalent quality of fit (Table 2).

Finally, we tried to improve the fit of the NPD data using z components for the four Fe magnetic moments. In order to decrease the number of free parameters, we used the previous Ho moment and retain only the Fe moments giving a calculated bulk magnetization close to its experimental value. As shown in Table 2, the fit is only slightly improved. Nevertheless, as shown in Fig. 4, only the "free canting" model correctly fit the small (1 1 3) peak, the ferrimagnetic model deviating hardly from the background. A vectorial diagram is shown in Fig. 4 for the deuteride results at 1.5 K. The mean canting angle θ between the Ho and resultant Fe moment is less than 10° as was found from magnetic measurements in hydrides.

The 1.5 K calculated mean Fe moment is close to 2.5 μ_B at.$^{-1}$ in deuteride and close to 1.85 μ_B at.$^{-1}$ in alloy. These values compare to those deduced from magnetization experiments: 2.27 μ_B at.$^{-1}$ and 2.02 μ_B at.$^{-1}$, respectively. This increase can be related to the increase of volume upon deuterium absorption: the Fe 3d bands are narrowed and Fe moments stabilized [10].

Concerning the Ho moment, both in deuteride and alloy its value is significantly less than its free ion value 10 μ_B at.$^{-1}$. This may be tentatively assigned to a magnetic contribution from the yttrium atom which was previously assumed to explain the neutron diffraction results observed in Y_6Fe_{23} and Y_6Mn_{23} [11].

Table 2
x- and z-axis components of magnetic moments (Bohr magnetons) of the different atoms in $Ho_5YFe_{23}D_{16}$ and Ho_5YFe_{23} at 1.5 K

	Ferrimagnetic	Canting Ho sublattice	"Free canting" deuteride	"Free canting" alloy
Ho (24e)	−9.347	−9.27 (−0.42)	−9.27 (−0.42)	−7.114 (5.5)
Fe1 (4b)	4.100	4.09	3.917 (−0.031)	2.874 (−2.227)
Fe2 (24d)	2.582	2.593	2.502 (1.728)	0.702 (−2.833)
Fe3 (32f_1)	2.590	2.569	2.591 (−1.183)	2.724 (0.77)
Fe4 (32f_2)	2.110	2.098	2.114 (0.622)	1.074 (−2.274)
⟨Fe⟩	2.487	2.478	2.473	1.855
$\lvert M_{tot}\rvert$	10.46	10.84	10.88	7.55
θ (°)	0	2.6	3.3	9.4
R_{mag}	3.57	3.86	3.38	2.68

⟨Fe⟩ is the mean Fe magnetic moment, M_{tot} the bulk magnetization per one formula unit.

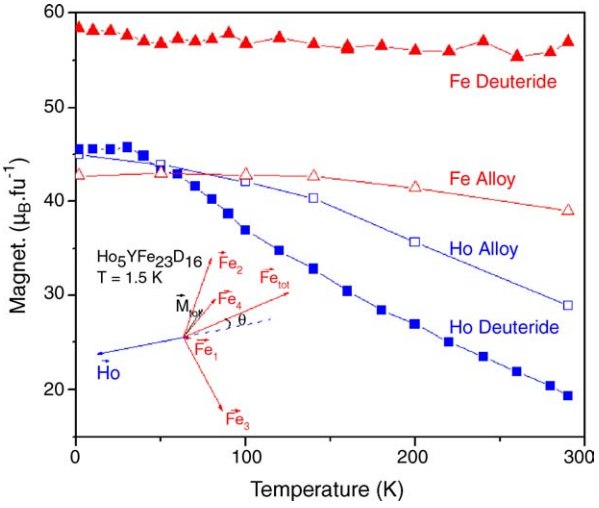

Fig. 4. Temperature variations of the Ho and Fe sublattices magnetizations for $Ho_5YFe_{23}D_{16}$ and its parent alloy according to the free canting angles modelization of the NPD data. Inset: the vectors diagram corresponds to 1.5 K free canting angles NPD fit for $Ho_5YFe_{23}D_{16}$. Fe_{tot} refers to the sum (per 1 f.u.) of the four Fe sublattices vectors; M_{tot} is the resultant magnetization of the compound.

We refine in the same manner the different NPD patterns of both $Ho_5YFe_{23}D_{16}$ and Ho_5YFe_{23} for all temperatures. The temperature variation of the Ho sublattice and of the resultant mean Fe sublattice moments for both compounds is reported in Fig. 4. Starting from the same value at 1.5 K, the temperature variation of the Ho moment is different in the deuteride and the alloy: the decrease is more important in the deuteride as compared to its parent alloy in spite of the fact that, due partly to the greater Fe moment, the Curie temperature is greater for the deuteride than for the alloy. This indicates that the magnetic interaction Ho–Fe is reduced in the deuteride as compared to its value in the alloy. A similar result was obtained in previous works [12]. This may be explained by the increase of the distance between the Ho magnetic rare-earth and its surrounding Fe neighbours in deuteride as compared to the alloy.

4. Conclusion

Upon hydrogenation, the mean Fe moment increases significantly as compared to its value in the alloy while due in part to the increase of the Ho–Fe distances, the magnetic interaction Ho–Fe decreases. NPD refinements are more in agreement with a slight mean canting angle ($\theta < 10^\circ$) than pure ferrimagnetism which is consistent with magnetization results, although it is not possible to determine precisely its value particularly for canting assumed in each Fe sublattice.

References

[1] E. Burzo, A. Chelkowski, H.R. Kirchmayr, H.P.J. Wijn (Eds.), Landolt-Börnstein Group III, vol. 19-d2, Springer, Berlin, 1990.
[2] M.B. Harris, G.A. Stewart, D.C. Creagh, Solid State Commun. 85 (1993) 389.
[3] J. Ostoréro, V. Paul-Boncour, J. Solid State Chem. 171 (2003) 334.
[4] J. Ostoréro, J. Alloys Compd. 317–318 (2001) 450.
[5] J.F. Herbst, J.J. Croat, J. Appl. Phys. 55 (1984) 3023.
[6] J. Rodriguez-Carvajal, Physica B 192 (1993) 55.
[7] J.J. Rhyne, K. Hardman-Rhyne, H.K. Smith, W.E. Wallace, J. Less Common Met. 94 (1983) 95.
[8] D.G. Westlake, J. Mater. Sci. 18 (1983) 605.
[9] E. Gratz, S. Markosyan, J. Phys. Condens. Matter 13 (2001) R385.
[10] S.F. Matar, V. Paul-Boncour, C.R. Acad. Sci. Paris IIc 3 (2000) 27.
[11] K. Hardman, W.J. James, W. Yelon, The Rare Earth in Modern Science and Technology, Plenum Press, New York, 1978, p. 403.
[12] F. Ishikawa, I. Yamamoto, M. Yamaguchi, M.I. Bartashevich, T. Goto, J. Alloys Compd. 253–254 (1997) 350.